HHS Public Access

Author manuscript

Virology. Author manuscript; available in PMC 2024 January 01.

Published in final edited form as:

Virology. 2023 January ; 578: 117–127. doi:10.1016/j.virol.2022.11.011.

SNAP23 is essential for germination of EV-D68 replication organelles

Katelyn Miller[1], **Michael A. Wagner**[1], **Alagie Jassey**[1], **William T. Jackson**[1,*]

[1]Department of Microbiology and Immunology, University of Maryland School of Medicine, 685 W Baltimore St. Baltimore, MD 21201

Abstract

Picornaviruses rearrange host cell membranes to facilitate their own replication. Here we investigate the Qbc SNARE, SNAP23, which is found at the plasma membrane and plays roles in exocytosis. We found that knockdown of SNAP23 expression inhibits virus replication but not release from cells. Knocking down SNAP23 inhibits viral RNA replication and synthesis of structural proteins. Normal cellular levels of SNAP23 are required for an early step in virus production, prior to or at the stage of virus RNA replication. We report that SNAP23 knockdown generates large, electron-light structures, and that infection of cells with these structures does not alter them, and those cells fail to generate viral RNA replication sites. We suggest that SNAP23 may play a role in maintaining membranes and lipids needed for generating virus replication organelles. Further investigation is needed to determine the precise role of this crucial SNARE protein in EV-D68 replication.

Keywords

picornavirus; SNARE; EV-D68; SNAP23

1. Introduction

Enterovirus D68 (EV-D68) is a severe respiratory virus of children, and biennial outbreaks of the virus have increased in severity over the past decade (Messacar et al., 2016). EV-D68

*Corresponding author. wjackson@som.umaryland.edu.

Declaration of interests

The authors declare that they have no known competing financial interests or personal relationships that could have appeared to influence the work reported in this paper.

CRediT Author Statement

Katelyn Miller: Conceptualization, Methodology, Validation, Formal analysis, Investigation, Writing - Original Draft, Writing - Review & Editing, Visualization, Project administration.

Michael Wagner: Conceptualization, Methodology, Validation, Writing - Review & Editing.

Alagie Jassey: Conceptualization, Methodology, Validation, Writing - Review & Editing.

William Jackson: Conceptualization, Methodology, Formal analysis, Writing - Original Draft, Writing - Review & Editing, Visualization, Supervision, Project administration, Funding acquisition.

has also emerged as a leading candidate explaining outbreaks of Acute Flaccid Myelitis (AFM), which have coincided with peak circulation of EV-D68, and several AFM patients have tested positive for EV-D68 (Messacar et al., 2018). Although there has been little study of the basic life cycle of EV-D68, our group and others have built on decades of study of other picornaviruses and found remarkable similarities in the way EV-D68 rearranges cellular membranes and interacts with host innate immune responses, including the autophagy pathway (Corona et al., 2018).

Autophagy, which is a constitutive cellular pathway of degradation, protein and organelle turnover, acts as an innate immune response against many viruses (Jackson, 2015; Karanasios and Ktistakis, 2016). However, for many positive sense RNA viruses, autophagy promotes virus replication. For many picornaviruses, our work and the work of others have led to a model in which autophagosome-like double-membraned vesicles can act as a harbor for maturation of the virion and subsequent release of vesicles filled with multiple virions (Chen et al., 2015; Feng et al., 2013; Richards and Jackson, 2012; Tabor-Godwin et al., 2012).

Autophagosomes would be expected to deliver their contents to lysosomes for degradation. However, that is clearly not the case, since the viruses benefit from autophagy and are not destroyed. Recently, we addressed this question in a study on autophagy and enterovirus D68 (EV-D68), a respiratory pathogen of children which has been implicated in outbreaks of Acute Flaccid Myelitis over the last decade (Messacar et al., 2018). Several pathogens, including RNA viruses, benefit from cellular mechanisms like macroautophagy (Wong and Sanyal, 2020). Our lab previously identified the importance of two human Qbc SNARE proteins, SNAP29 and SNAP47, in autophagy-mediated EV-D68 replication. SNARE (soluble N-ethylmaleimide-sensitive factor-attachment protein (SNAP) receptor) proteins are categorized as Q-SNAREs or R-SNAREs depending if a glutamine (Q) or arginine (R) residue contributes to the protein complex. Q-SNAREs are further organized as Qa, Qb, and Qc depending on the location of the glutamine residue on the SNARE complex. Qbc SNARES contribute two coiled-coil domains to SNARE complexes, with glutamine residues in the b and c positions (Margiotta 2022). EV-D68 cleaves the SNAP29 protein, a soluble N-ethylmaleimide-sensitive factor attachment protein receptor (SNARE) thought to be responsible for autophagic fusion events (Corona et al., 2018). Another enterovirus, Coxsackievirus B3, also cleaves SNAP29, indicating this is a common target for these viruses (Mohamud et al., 2018). SNAP29, which is not membrane-associated, has been identified as a key autophagic fusion adapter (Itakura and Mizushima, 2013; Morelli et al., 2014). SNAP29 has two coiled-coil binding domains and forms a complex with two other SNARE proteins: STX17, which is found on immature autophagosomes; and VAMP8, which is found on lysosomes. Cleavage of SNAP29 by viral proteases separates the STX17-binding domain from the VAMP8-binding domain, suggesting potent dominant negative functions for the cleaved products in preventing delivery of virus-containing autophagosomes to lysosomes.

Another Qbc SNARE, SNAP23, and its relationship and role with EV-D68 replication has yet to be fully investigated. SNAP23 is a plasma membrane-associated vesicle fusion protein that largely plays a role in the regulation of docking and fusion of transport vesicles and

is associated with exocytosis. Various studies have shown that replication in both DNA and RNA human viruses have been affected by interactions with SNARE proteins (Ding et al., 2014; Liu et al., 2011; Ren et al., 2016). SNAP23 is known to be involved with exocytosis for different cell types (Hatsuzawa and Sakurai, 2020; Zylbersztejn and Galli, 2011). In relation to viral exit, it has recently been reported that the SNAP23 neuronal homolog, SNAP25, plays an important role in Rabies virus egress in nerve cells (Yin et al., 2020). With these factors in mind and the overall known functions of SNAP23, we hypothesized that it might be involved with the viral life cycle at the plasma membrane, such as binding and entry of virions, or trafficking newly formed mature EV-D68 virions to the plasma membrane for nonlytic egress. Here we investigated the role of SNAP23 in the EV-D68 life cycle, and we present our findings that SNAP23 is required early in the viral life cycle. Our data suggest that SNAP23 maintains cellular resources that are needed upon infection to germinate viral RNA replication complexes.

2. Materials and Methods

Cells and Viruses

H1HeLa cells were cultured in MEM supplemented with 10% fetal bovine serum (FBS) and sodium pyruvate (1X final concentration). The H1HeLa cell line was obtained from ATCC. Virus was produced through *in vitro* transcription of viral cDNA and RNA transfection into HeLa cells. Plaque picks from transfection were expanded no more than two times to produce working virus stock. H1HeLa cells were seeded one day prior to infection. The day of infections, cells were counted and EV-D68 infections were carried out using multiplicity of infections (MOIs) of 0.1, 10, 25, or 30 (as indicated in the figure legends). Virus stock was diluted in PBS+ (1X phosphate buffered saline (PBS) containing magnesium chloride and calcium chloride), added dropwise to cells, and incubated at 37°C for 30 minutes, unless otherwise indicated in the figure legends or methods section. After adsorption incubation, virus dilution was aspirated and cells were washed three times with 1X PBS to remove unbound virus before complete media was added to cells. Experiments that involved inhibiting EV-D68 replication used guanadine hydrochloride (GuHCl) (G3272, Sigma-Aldrich) at a final concentration of 2 mM. GuHCl was added to the media immediately after viral adsorption or at indicated timepoints.

SDS-PAGE and Western Blot

For each sample, media was aspirated and cells were washed with PBS. Cells were scraped and collected in fresh PBS and centrifuged at 12,000–15,000 rpm for 5 minutes. The supernatant was aspirated off, leaving the cell pellet. Each pellet was lysed in RSB(resuspension buffer)-NP40, containing 10 mM Tris-HCl (pH 7.5), 10 mM sodium chloride, 1.5 mM magnesium chloride, 1% NP-40, and protease inhibitor. Samples were kept on ice for 30 minutes before measuring for protein concentration. Protein concentration was measured using bovine serum albumin standards and Bradford Reagent (B6916, Sigma-Aldrich).

Each sample was boiled for 15 minutes and subjected to SDS-PAGE on a 12% gel at 90V until samples ran completely through the stacking gel, then 125V for the remainder

of the gel. Samples were transferred to a PVDF membrane using the iBLOT2 transfer system. Blots were blocked in 5% milk-TBST (tris-buffered saline with Tween20) for 1 hour at room temperature (RT). Primary antibodies were diluted at 1:1000–1:5000 in 1% milk-TBST overnight at 4°C. Primary antibodies used include: SNAP23 ([EPR8538], ab131242, Abcam), LC3 (NB600-1384, Novus), SQSTM1 (H00008878-M01, Abnova), Beta Actin (NB600-532, Novus), and Enterovirus pan Monoclonal Antibody to detect VP3 (MA5-18206, Invitrogen). Blots were washed three times in 1X TBST for 10 minutes. Secondary antibodies (Goat Anti-Mouse IgG (H + L)-HRP Conjugate, BIO-RAD #1706516 and Goat Anti-Rabbit IgG (H + L)-HRP Conjugate, BIO-RAD #1706515) were diluted at 1:2000–1:10000 in 1% milk-TBST and incubated at RT for 1 hour while on a shaker. After secondary antibody incubation, blots were washed three times with 1X TBST for 10 minutes each wash. A 1:1 ratio of Western Light Plus-ECL (enhanced chemiluminescence substrate) was mixed (PerkinElmer, Inc.) and used prior to blot imaging. Blots were imaged using a Bio-Rad ChemiDoc and the Bio-Rad Image Lab (version 6.1) program.

Plaque Assay

Extracellular samples (1 mL of conditioned media) and intracellular samples (cells scraped in 1 mL of PBS+) were collected. Samples were freeze/thawed in a dry ice/ethanol bath three times. Samples were then serially diluted in PBS+. Desired dilutions were added to 60 mm dishes or 6-well dishes containing 100% confluent H1HeLa cells and adsorbed for 30 minutes at 37°C. After adsorption, an agar overlay (1:1 ratio of 2X MEM and 2% bactoagar) was added to each dish or well. After the overlay solidified, samples were incubated at 37°C for up to 48 hours or until plaques formed. The agar overlay was removed and stained in 1% crystal violet.

Immunofluorescence Microscopy

Cells were seeded on 18 mm coverslips a day before infection. After the infection, coverslips were fixed in 4% paraformaldehyde for 15 minutes and washed three times with 1X PBS for 5 minutes each. Samples were then blocked with a blocking buffer (1X PBS/5% normal goat serum/0.1% saponin) for 1 hour at RT, while on a shaker. After blocking, primary antibody for SNAP23 (ab3340, Abcam), VP3 (MA5-18206, Invitrogen), or dsRNA (SIG-MABE1134, Sigma) at a 1:200 dilution was added to each coverslip and incubated overnight at 4°C. The following day, coverslips were washed three times in 1X PBS for 5 minutes each. Secondary antibody (Alexa Fluor 488 or Alexa Fluor 594) was applied to coverslips at RT for 1 hour. Samples were washed three times with 1X PBS before mounting on microscope slides using ProLong Glass Antifade Mountant (P36985, Invitrogen) with NucBlue (Hoescht). Coverslips were allowed to cure overnight at RT before storing at 4°C. Images were acquired using the Echo Revolve microscope and analyzed using FIJI.

siRNA Knockdowns

Transient SNAP23 and control knockdowns were performed using Lipofectamine 2000 (Thermo Fisher) per the manufacturer's protocol. Non-targeting siRNA and a pool of three SNAP23 siRNAs (Millipore Sigma: SASI_Hs01_00224584: 5'-CGUAGCUCCUCCUUGAAAG-3' 5'-CUUUCAAGGAGGAGCUACG-3', SASI_Hs01_00224583:5'-

CUAAUUGGGAGAUAAUAUG-3'5'-CAUAUUAUCUCCCAAUUAG-3', and SASI_Hs01_00172213:5'-CUAAUUGGGAGAUAAUAUG-3' 5'-CUUUCAAGGAGGAGCUACG-3') were individually resuspended in annealing buffer, boiled for 5 minutes, and incubated for one hour at 37°C (stock concentration at 100 μM). The day before transfection, cells were seeded so that they would be 30–50% confluent. Lipofectamine 2000 and siRNAs were diluted in Opti-MEM™ I Reduced Serum Medium (Gibco), combined and incubated at RT for 20 minutes, and then added to cells dropwise. Cells were then transfected for 48 hours at 37°C. After 48 hours, samples were subjected to EV-D68 infection.

Attachment and Entry Assays

After 48 hours of SNAP23 siRNA knockdown or non-targeting siRNA, H1HeLa cells were pre-chilled at 4°C for 1 hour. Cells were washed with ice cold 1X PBS before the addition of virus adsorption media (PBS+) at an MOI of 30 for 1 hour at 4°C. After adsorption, cells were washed three times with ice cold 1X PBS to wash off unbound virus. Samples to assess attachment were collected in PBS+ after the PBS wash. Complete media was added to samples and incubated at 37°C for 1 hour to assess viral entry. After incubation, samples were washed with 1X PBS three times and collected in PBS+. Samples for attachment and entry were freeze thawed three times before determining virus titer by plaque assay.

Cysteine Mutant and Transfection to Target SNAP23 Palmitoylation

Primers were designed to create mutant versions of SNAP23 targeting cysteine residues and substituting with nucleotides that correspond to either alanine or leucine. Site-directed mutagenesis by PCR was used to create several constructs. Mutagenesis was done using the pEGFP-SNAP23 plasmid (Addgene, Plasmid #101914) and custom primers (Sigma-Aldrich). Primers for the C80A mutation are as followed: forward 5'-CTCAACAAATGCGCAGGCCTTTGTGTCTGC-3' and reverse 5'-CATGGGCAGACACAAAGGCCTGCGCATTT-3'. Constructs were transformed into DH5α competent cells (Invitrogen). Individual colonies were picked and then used for DNA sequencing. Each construct was verified via sequencing (Genewiz). Sequences were subsequently aligned to the original EGFP-SNAP23 sequence to verify the introduction to the desired mutation. Selected mutant constructs were then amplified using MAXI Prep (Qiagen) and measured DNA concentration using a DeNovix spectrophotometer.

DNA Transfections

Transfections of C1-GFP, pEGFP-SNAP23 plasmid and the cysteine mutant were carried out using Lipofectamine 2000 in H1HeLa cells. H1HeLa cells were seeded onto 60 mm dishes the day prior to yield 80–90% confluency the day of transfection. Preliminary tests optimized using 8 μL of lipofectamine and 4 μg of DNA per 60 mm dish to ensure cell viability and appropriate transfection efficiency. Four hours post transfection, cells were seeded to either 18 mm glass coverslips or 6-well plates. 20 hours post transfection, cells were infected with EV-D68 at high or low MOI at various time points as indicated in each experiment.

RNA Isolation, cDNA Synthesis, and Quantitative Polymerase Chain Reaction (qPCR)

Total RNA was collected from infected H1HeLa cells after each time point with TRIzol™ Reagent (Ambion, 15596026) using the manufacturer's protocol. RNA quality and quantity was checked using a DeNovix spectrophotometer. After removing genomic DNA, cDNA was synthesized using the RevertAid H Minus First Strand cDNA Synthesis Kit (Thermo Scientific, K1632). KiCqStart SYBR qPCR Ready Mix (Sigma, KCQS01) and 7500 Fast Dx Real-Time PCR Instrument (Applied Biosystems) were used for qPCR. GAPDH primers were used as our control and primers for the 5'UTR of EV-D68 (5′ TAACCCGTGTGTAGCTTGG-3′ and 5′ -ATTAGCCGCATTCAGGGGC-3′) were used for EV-D68 amplification. All non-targeting and siSNAP23 gene expression results were normalized to GAPDH and $2^{-\Delta\Delta CT}$ values were compared to non-targeting 0 hours post infection (hpi). Values were then log transformed before statistical analysis.

Transmission Electron Microscopy

Non-targeting and siSNAP23 knockdown H1HeLa cells were infected with EV-D68 (MOI = 10) or mock infected for 4 hours. Samples were then prepared, sliced, and imaged using the Electron Microscopy Core Imaging Facility at the University of Maryland, Baltimore. Cells were fixed with a solution of 2% paraformaldehyde, 2.5% glutaraldehyde in 0.1 M PIPES buffer (pH 7.2), scrapped off the tissue culture plate, washed in 0.1M PIPES buffer, and collected by centrifugation. Cell pellets were enrobed in 2.5% low melting point agarose, trimmed into 1mm3 blocks and post-fixed with 1% osmium tetroxide and 1.5% potassium ferrocyanide in 0.1M PIPES buffer for 1 hour at 4°C. After washing, agarose blocks containing cells were en bloc stained with 1% uranyl acetate in water and dehydrated using increasing concentration of ethanol from 30%; 50%; 70%; 90% and 100% for 10 min at each step. Specimen were then incubated with two changes of 100% acetone and infiltrated, in increasing concentration of Araldite-Epoxy resin (Araldite, EMbed 812; Electron Microscopy Sciences, PA), and embedded in pure resin at 60°C for 24 to 48 h. Ultrathin sections at ~70nm thickness were cut on Leica UC6 ultramicrotome (Leica Microsystems, Inc., Bannockburn, IL). Images were taken using a FEI Tecnai T12.

Statistical Analysis

Virus titers were assessed and analyzed by using a student T-test. Each experiment was conducted independently at least three times, unless otherwise indicated in the figure legends. Statistical analysis and graphs were generated using GraphPad PRISM (9.4.1). * indicated a p-value less than 0.05.

3. Results

The Effects of EV-D68 Infection on SNAP23 Localization

To better understand the relationship between SNAP23 and the EV-D68 life cycle, we began by investigating the effects of EV-D68 infection on SNAP23 localization. SNAP23 is known to localize to the inner leaflet of the plasma membrane and play a role in exocytosis (Kubo et al., 2015). To analyze SNAP23 localization, H1HeLa cells were infected with EV-D68, at an MOI of 25, for 0, 2, 3, 4, and 5 hours. At each indicated time point, cells were fixed and

prepared for immunofluorescence staining against endogenous SNAP23 (green) and viral capsid protein VP3 (red) (Figure 1A). We observed SNAP23 ubiquitously expressed and localized at the plasma membrane and in the cytoplasm in mock infected cells, 0 hpi, and 2 hpi. At the mock and 0 hpi timepoint, VP3 was yet to be expressed, as we expect since the peak of viral replication occurs roughly at 3 hpi. SNAP23 is no longer associated with the plasma membrane at 3, 4, and 5 hpi, when compared to the mock infection. By 3 hpi and beyond, VP3 was readily expressed throughout the cells. Cells started to show signs of cytopathic effects at 5 hpi, with condensed nuclei and cell rounding. Although both SNAP23 and VP3 were expressed throughout the cytoplasm, the two proteins did not significantly co-localize.

We further observed SNAP23 re-localization to the cytosol during EV-D68 infection, does require active viral replication. Guanadine hydrochoride (GuHCl; final concentration 2 mM) was added to the media at 0 hpi or 1 hpi. Viral infection continued for five hours as performed in Figure 1A. As we showed during mock infection and 0 hpi, SNAP23 localized to the plasma membrane, whereas at the end of a 5 hour infection, SNAP23 primarily resided at the cytosol (Figure 1B). GuHCl treated cells, however, retained SNAP23 localization to the plasma membrane (Figure 1B). These results indicate that active EV-D68 replication leads to relocalization to the cytosol for this plasma membrane protein.

SNAP23 Expression is not Altered by EV-D68 Infection but SNAP23 Knockdown Inhibits VP3 Expression

Although we could detect localization changes, we were unsure from immunofluorescence studies if EV-D68 infection affects overall SNAP23 expression. Cells were infected with EV-D68 (MOI=25) and lysates collected at 0, 1, 2, 3, 4, or 5 hours. VP3 expression during a normal infection was detectable starting at 3 hours of infection, as shown in Figure 1. SNAP23 expression, overall, did not significantly change over the course of a 5 hour infection when compared to the mock infection (Figure 2A and 2C). This was somewhat surprising, since in our previous studies, EV-D68 infection reduced SNAP47 protein levels and resulted in the cleavage of SNAP29 by viral protease 3C (Corona et al., 2018). LC3-I, LC3-II and SQSTM1 were also assessed to verify autophagic marker changes known to be induced during EV-D68 infection. As with previous studies, we observed lipidation of LC3-I to LC3-II and reduction of SQSTM1 levels at 4 hpi and 5 hpi (Figure 2A). Steady-state levels of SQSTM1, an autophagy cargo adapter protein, drop during active autophagic degradation. Overall, these results indicate that EV-D68 infection itself is not altering levels of SNAP23 expression nor cleaving the protein during infection, as observed for other Qbc SNAREs SNAP47 and SNAP29 (Corona et al., 2018).

To further confirm the importance of SNAP23 in the EV-D68 replication cycle, we assessed expression of viral capsid protein VP3 during infection under SNAP23 knockdown conditions. H1HeLa cells were transfected for 48 hours with siRNAs for SNAP23 or non-targeting control as described previously. After 48 hours, cells were infected with EV-D68 or mock infected for 4 hours at an MOI of 10. We chose this time point to ensure cell viability, but also to ensure detectable expression of VP3. Guanidine hydrochloride (GuHCl) is commonly used to inhibit picornavirus RNA replication, and prevented production of

VP3 during infection (Figure 2B). We observed an overall trend of increased levels of the full length SQSTM1 autophagy marker in knockdown cells compared to the non-targeting control (Figure 2B, 2D). Our lab and others have shown that SQSTM1 is cleaved by viral protease 3C (Shi et al. 2013; Shi et al. 2014; Corona et al. 2018). In SNAP23 knockdown cells infected with EV-D68, SQSTM1 cleavage was reduced in comparison to the non-targeting control (Figure 2B, arrow), further confirming that loss of SNAP23 affects EV-D68's ability to interact with the host cell machinery to enhance viral replication. Together, our results support the idea that EV-D68 requires endogenous levels of SNAP23 for normal virus production. Since levels of the viral structural protein VP3 were reduced in SNAP23 knockdown cells, we considered a role for SNAP23 early in the life cycle EV-D68.

SNAP23 Knockdown Affects EV-D68 Replication, but not Viral Release

Previous studies in our lab investigated the roles of two Qbc SNARES, SNAP29 and SNAP47, in EV-D68 infection (Corona et al., 2018). SNAP29 is required for early replication, with siRNA knockdown of SNAP29 resulting in decreased virus titer. However, SNAP29 is then cleaved by viral protease 3C during late stages of replication, suggesting that it is either unnecessary or inhibitory later in the virus life cycle. SNAP47's role in EV-D68 replication appears to be during later stages of the infection cycle. The current hypothesis is that SNAP47 promotes acidification of autophagosomes, which is necessary for EV-D68 replication. First, we needed to understand if SNAP23 is important for virus replication.

H1HeLa cells were transfected for 48 hours with either non-targeting siRNA or a pool of three SNAP23 targeting sequences. After 48 hours, cells were infected with EV-D68 at an MOI of 0.1 for 6 hours. Intracellular and extracellular (conditioned media) samples were analyzed for virus titer levels by plaque assay. Knockdown of SNAP23, in line with SNAP29 and SNAP47 knockdowns, significantly decreased intracellular virus titer, a bit more than two-fold, in comparison to the non-targeting control (Figure 3A). However, unlike the SNAP29 and SNAP47 knockdowns, the extracellular samples of SNAP23 knockdown samples showed no significant change in virus titer levels (Figure 3B). SNAP23 knockdown efficiency was confirmed by Western blot analysis (Figure 3C). These results are in line with the reduction of VP3 expression in SNAP23 knockdown cells infected with EV-D68 (Figure 2B). To investigate the effect of overexpression of this protein on virus production, we transfected cells with an EGFP plasmid (C1) as a control, or a plasmid expressing EGFP fusions of either wild type SNAP23 or SNAP23 containing a mutation (C80A) that was previously shown to eliminate membrane localization of the protein (Agarwal et al., 2019). H1HeLas were transfected for 20 hours then infected with EV-D68 for 6 hours at an MOI of 0.1. We found there were no statistically significant changes between intracellular (Figure 3D) and extracellular (Figure 3E) titers when compared to cells that were only transfected with the EGFP control. However, we did notice a slight trend that showed eGFP-SNAP23 overexpressing cells decreased intracellular virus titer by roughly two-fold in comparison to the EGFP only control. We believe homeostatic levels of SNAP23 may be required for efficient viral replication. Together, the data suggest that SNAP23, like the other Qbc SNARE proteins we investigated, is required for EV-D68 replication, but also imply that SNAP23 primarily affects steps of the viral life cycle that occur before viral exit.

SNAP23 Knockdown Affects EV-D68 Post-Entry

SNAP23 is widely associated with the plasma membrane and processes such as exocytosis. However, we have shown that overexpressing or knocking down SNAP23 does not affect EV-D68 egress from the cell (Figure 3). As seen in Figure 1, SNAP23 localizes to the inner leaflet of the plasma membrane early in infection, so we theorized it might be involved in virion binding or entry.

After SNAP23 or control knockdowns, we performed attachment and entry assays (see full description in the materials and methods), collected samples, and compared intracellular titers to the non-targeting control by plaque assay. We found that both conditions yielded similar titers as the input amount of virus during adsorption, and thus there was no significant effect on EV-D68 attachment when SNAP23 was knocked down (Figure 4A). Similarly, we found there was no statistical significance when we assessed for viral entry (Figure 4B). These results suggest that, despite the evidence that SNAP23 is associated with the plasma membrane, the role of SNAP23 during EV-D68 infection and life cycle is not associated with viral processes associated with the plasma membrane, such as attachment, entry, and exit. Instead, we believe SNAP23 must be involved with processes associated with the cytosol, such as active replication of the virus.

We next performed a full time course of infection after SNAP23 knockdown, infecting cells at MOI of 0.1 to identify the timing and magnitude of the effect on virus titer. Intracellular viral titers in SNAP23 knockdowns decrease by about half of a log starting at 3 hpi, 4 hpi, and 5 hpi (Figure 4C), although these differences are not statistically significant until 6 hpi. These results suggest that the role of SNAP23 in the life cycle is revealed starting at the peak of vRNA replication (3 hpi). We confirmed these findings by qPCR. We chose primers for the 5’UTR of EV-D68 and compared non-targeting control infected samples to siSNAP23 infected samples over a time course (0, 1.5, 3, and 5 hpi) at an MOI of 10. All samples were normalized to GAPDH, values for $2^{-\Delta\Delta CT}$ were calculated, compared to the 0 hpi of the non-targeting control, and were log transformed before undergoing statistical analysis. Similar to our titer data, we found that starting at 3 hpi, viral RNA levels were downregulated compared to the non-targeting control, and reached significance by 5 hpi (Figure 4D). Therefore SNAP23 affects EV-D68 replication post-entry, but before significant RNA replication occurs. Since viral genomic RNA levels were reduced in SNAP23 knockdown cells, we next considered a role for SNAP23 in viral RNA replication.

SNAP23 is Necessary for Viral RNA Replication

Under mock conditions, we were able to identify and distinguish cells that were knocked down for SNAP23. SNAP23 (green) was ubiquitously expressed in the cytoplasm in non-targeting siRNA conditions, whereas in knockdown conditions, the remaining SNAP23 signal was mostly localized to the nucleus or perinuclear region of the cell (Figure 5A). Similar to our Western blot results in Figure 2B, cells transfected with non-targeting siRNAs and infected with EV-D68 showed prominent expression of VP3 (red), whereas cells transfected with SNAP23 siRNAs and infected had noticeably reduced levels of expression (Figure 5A). Under the same knockdown conditions, we also investigated the production of double stranded RNA (dsRNA). dsRNA is an intermediate synthesized during active viral

RNA replication and can be used as a replication marker. We found that most non-targeting siRNA transfected cells that were infected with EV-D68 (MOI = 10) expressed dsRNA puncta at 5 hpi (Figure 5B). In contrast, siSNAP23 transfected cells showed noticeably fewer cells that displayed dsRNA puncta at that same timepoint (Figure 5B). Subsequently, the cells with most SNAP23 staining within the cytosol tended to have the most dsRNA staining (Figure 5B; white dotted selection).

We noticed an interesting phenotype when we used siRNA to knockdown SNAP23. Under phase contrast light microscopy, we observed circular, light spaces in the cytoplasm of SNAP23 siRNA transfected cells (Figure 5D), in contrast to the non-targeting control (Figure 5C). Using immunofluorescence microscopy, when staining for SNAP23 we identified circular, cytosolic rings of SNAP23 (Figure 5F, arrows) which are absent in cells with the non-targeting control (Figure 5E). We have also observed immunofluorescent staining for SNAP23 to be substantially absent in the cytosol during the knockdown conditions (Supplemental Figure 1). Therefore we wanted to explore the structural changes on the cell during SNAP23 knockdown using transmission electron microscopy (TEM).

SNAP23 Knockdown Generates Large Vacuoles and Occludes Formation of Viral Replication Organelles.

To investigate the structural changes during SNAP23 knockdown, we compared cells with non-targeting siRNA or SNAP23 siRNA and mock infection to non-targeting siRNA or SNAP23 siRNA with a 4 hour EV-D68 infection condition (MOI=10). Cells were fixed and prepared for TEM imaging (see Materials and Methods). We observed normal organelle development and overall normal cell morphology in cells transfected with non-targeting siRNA with mock infection (Figure 6). In contrast, we noticed cells that were transfected with the SNAP23 siRNA exhibiting a similar phenotype in phase contrast and immunofluorescence images, with large unstained/empty spaces found within the cell (Figure 5D and 5F). Upon infection, cells transfected with non-targeting siRNA showed typical characteristics of picornavirus infection, including membrane and organelle rearrangement resulting in membranous structures known as replication organelles (Figure 6, red circles)(Hsu et al. 2010). These organelles are the physical site of viral RNA replication. However, cells that were infected with EV-D68 and transfected with SNAP23 siRNAs exhibited the same electron light/empty vacuoles, but showed little to no formation of replication organelles (Figure 6). Together these results strongly suggest that SNAP23 is able to direct active viral RNA replication by promoting the formation of viral RNA replication organelles.

4. Discussion

SNAP23 is known to play a role in exocytosis and to localize at the plasma membrane (Kubo et al., 2015). Therefore, our original hypothesis was that SNAP23 would play a role in the EV-D68 life cycle at a stage associated with the plasma membrane, such as viral entry or virion release. However, when we overexpressed or depleted SNAP23, there was no effect on released virus. We also observed during infection that SNAP23 localization changed during infection, with the protein’s association with the plasma membrane diminishing at

later time points of infection (Figure 1). Given these results, we examined early stages of the viral life cycle, such as viral attachment and entry. Our results revealed that endogenous levels of SNAP23 are in fact crucial at an early point in viral replication. However, our data exclude viral entry and led us to the conclusion that SNAP23 is involved in the process of synthesizing viral RNA replication organelles.

Knockdown of SNAP23 by siRNA lowered intracellular virus titer (Figure 3A). Reduction of virus production as a result of SNAP23 knockdown has also been observed with human cytomegalovirus (HCMV) (Liu et al., 2011). The reduction in EV-D68 replication also coincides with results our group has previously published on Qbc SNARES, in which knockdown of either SNAP29 or SNAP47 resulted in decreased EV-D68 replication (Corona et al., 2018). Studies of Coxsackievirus 3B have shown that knockdown of SNAP29 resulted in increased intracellular virus (Mohamud et al., 2018). When H1HeLa cells were transfected to overexpress SNAP23, both intracellular and extracellular EV-D68 levels were not significantly affected in comparison to cells transfected with the GFP control (Figure 3D and 3E). However, it is interesting to note that GFP-SNAP23 transfected cells showed reduced intracellular titer in comparison to the GFP control, similar to what we see in SNAP23 knockdown conditions. This indicates the likely importance of homeostatic levels of SNAP23 for efficient EV-D68 replication. Therefore, we conclude that SNAP23 has little effect on virus release. This contrasts the results when SNAP29 is overexpressed, with increased virus levels released into the media (Corona et al., 2018). We believe that the capacity of non-lytic release mechanisms, such as AWOL (Autophagic exit WithOut Lysis) is likely far below the amount of virus available in the cytoplasm (Jackson et al. 2005). Therefore, reducing the amount of intracellular virus produced does not immediately reduce the amount of non-lytic release.

In our previous study, EV-D68 infection induced cleavage of SNAP29 or a decrease in SNAP47 protein levels. In contrast, SNAP23 protein expression was not significantly affected with EV-D68 infection (Figure 2A). Similarly, it has been shown that SNAP23 expression is not affected by infection of a related picornavirus, coxsackievirus B3 (Xiang et al. 2021). Thus, the protein appears to be maintained at normal intracellular levels during EV-D68 infection.

When SNAP23 was knocked down, EV-D68 was able to bind, attach, and enter cells as effectively as the non-targeting control (Figure 4A and 4B). However, post-entry events in the EV-D68 life cycle were impacted by knocking down SNAP23. The expression of the structural protein VP3 is greatly inhibited when compared to the non-targeting control, as seen by immunofluorescence microscopy and Western blot analysis (Figures 2B and 5A). Knocking down SNAP23 also resulted in an interesting trend where we observed decreased intracellular virus titer, not only at the end of a single replication cycle (6 hours), but with a similar trend at 3, 4, and 5 hours post infection, though the difference was not statistically significant at earlier time points (Figure 4C). Similarly, we found that transcript levels of the 5’UTR of EV-D68 by qPCR were also affected when we knocked down SNAP23 (Figure 4D). Together, this shows that depletion of endogenous SNAP23 impacts the life cycle of EV-D68 at the level of vRNA production, with subsequent effects on viral protein translation and production of new virions. Although SNAP23 is best known to be associated with the

plasma membrane and exocytosis, the protein also has functions away from the plasma membrane involving endosomal fusion events (Klein et al. 2017; Valdez et al. 1999) and intracellular trafficking, most notably for phagosomes (Nair-Gupta et al. 2014; Sakurai et al. 2012; Hatsuzawa and Sakurai 2020; Dingjan et al. 2017). It has been established that host membranes are rearranged to support picornavirus RNA replication in unique virus-induced organelles (Belov et al., 2012; Richards et al., 2014). More recently, studies have shown that the formation of picornavirus replication organelles may require interactions with lipid droplets (Melia et al. 2019; Laufman et al. 2019). SNAP23 and other SNAREs have also been reported to have interactions with lipid droplets (Boström et al., 2007; Jägerström et al., 2009; Monteiro-Brás et al., 2019). Therefore we believe it is likely that SNAP23 is involved, possibly indirectly, in generating these RNA replication membrane structures.

Throughout our experiments we noticed when cells were knocked down for SNAP23, large vacuolar structures devoid of SNAP23 were observed in a large portion of cells (Figures 5D and 5F), whereas cells with non-targeting siRNA transfected did not (Figures 5C and 5E). Transmission electron microscopy revealed several cells with large electron-light structures when SNAP23 is knocked down (Figure 6). Subsequently, when cells were infected with EV-D68, we found that cells with these large structures did not form replication organelles. Cells transfected with non-targeting siRNA formed replication organelles that we typically see during EV-D68 infection or other picornavirus replication. Accordingly, we performed immunofluorescence microscopy and looked at dsRNA (an intermediate for active viral RNA replication). In comparison to the non-targeting control, where most cells were expressing dsRNA, we noticed cells that were knocked down for SNAP23 had noticeably fewer numbers of cells expressing dsRNA puncta (Figure 5B). We did not observe dsRNA directly co-localizing or overlapping with SNAP23, although the two signals are in proximity. However, SNAP23 expression is more diffuse than dsRNA and does not display distinct clusters of puncta. Collectively, this implies that normal levels of SNAP23 are necessary for the formation of viral RNA replication organelles in order for EV-D68 to effectively replicate in host cells. We suspect that SNAP23 must maintain host cell homeostasis in order for viral replication to take place. We suggest that when SNAP23 expression is depleted, defects in trafficking events result in the large vacuolar structures. The SNAP23-dependent resources required to form replication organelles are likely diverted into these large structures. We suggest these vacuoles may be This renders them unavailable to the virus, effectively stealing the membranes, lipids, or other resources needed to build vRNA replication organelles (Figure 7). mis-fused trafficking vesicles, unable to target normally in the absence of SNAP23. While SNAP23's role in endocytosis makes it tempting to predict that the large structures could be constructed from misdirected endosomes, inhibiting one pathway after affects others, so these could also be derived from exosomes, for example. Future studies are needed to better understand the intracellular roles of SNAP23 that provide materials for the germination of replication organelles during EV-D68 infection.

5. Conclusion

In summary, our study reveals SNAP23 plays an important role in replication or EV-D68 genomic RNA, specifically regulating the formation of replication organelles. Collectively,

our immunofluorescence and titer data further support that 1) SNAP23 plays a role in regulating EV-D68 replication and 2) SNAP23 levels must be maintained to provide membrane components needed for efficient viral replication. In the absence of SNAP23, cellular resources are diverted into large structures and made unavailable to generate replication organelles. Further experiments are necessary to understand the mechanism(s) and virus-host interactions behind these observations. Overall, our work has further contributed to the important role of SNARE proteins in viral replication.

Supplementary Material

Refer to Web version on PubMed Central for supplementary material.

Acknowledgements

We thank the Jackson and Frieman labs for discussion and assistance with this project. We thank the University of Maryland School of Medicine Center for Innovative Biomedical Resources, Electron Microscopy Core – Baltimore, Maryland for help with the EM work, which utilized a sample preparation instrument that was purchased with funding from an NIH SIG grant (1S10RR26870-1). W.T.J. was supported by NIH/NIAID grants R01AI104928 and R01AI141359. K.M was supported by NIH/NIAID grant T32AI095190.

References.

Agarwal V, Naskar P, Agasti S, Khurana GK, Vishwakarma P, Lynn AM, Roche PA, Puri N, 2019. The cysteine-rich domain of synaptosomal-associated protein of 23 kDa (SNAP-23) regulates its membrane association and regulated exocytosis from mast cells. Biochim. Biophys. Acta Mol. Cell Res. 1866, 1618–1633.

Belov GA, Nair V, Hansen BT, Hoyt FH, Fischer ER, Ehrenfeld E, 2012. Complex dynamic development of poliovirus membranous replication complexes. J. Virol. 86, 302–312. [PubMed: 22072780]

Boström P, Andersson L, Rutberg M, Perman J, Lidberg U, Johansson BR, Fernandez-Rodriguez J, Ericson J, Nilsson T, Borén J, Olofsson S-O, 2007. SNARE proteins mediate fusion between cytosolic lipid droplets and are implicated in insulin sensitivity. Nat. Cell Biol. 9, 1286–1293. [PubMed: 17922004]

Chen Y-H, Du W, Hagemeijer MC, Takvorian PM, Pau C, Cali A, Brantner CA, Stempinski ES, Connelly PS, Ma H-C, Jiang P, Wimmer E, Altan-Bonnet G, Altan-Bonnet N, 2015. Phosphatidylserine vesicles enable efficient en bloc transmission of enteroviruses. Cell 160, 619–630. [PubMed: 25679758]

Corona AK, Saulsbery HM, Corona Velazquez AF, Jackson WT, 2018. Enteroviruses Remodel Autophagic Trafficking through Regulation of Host SNARE Proteins to Promote Virus Replication and Cell Exit. Cell Rep. 22, 3304–3314. [PubMed: 29562185]

Ding B, Zhang G, Yang X, Zhang S, Chen L, Yan Q, Xu M, Banerjee AK, Chen M, 2014. Phosphoprotein of human parainfluenza virus type 3 blocks autophagosome-lysosome fusion to increase virus production. Cell Host Microbe 15, 564–577. [PubMed: 24832451]

Feng Z, Hensley L, McKnight KL, Hu F, Madden V, Ping L, Jeong S-H, Walker C, Lanford RE, Lemon SM, 2013. A pathogenic picornavirus acquires an envelope by hijacking cellular membranes. Nature 496, 367–371. [PubMed: 23542590]

Hatsuzawa K, Sakurai C, 2020. Regulatory Mechanism of SNAP23 in Phagosome Formation and Maturation. Yonago Acta Med. 63, 135–145. [PubMed: 32884432]

Itakura E, Mizushima N, 2013. Syntaxin 17: the autophagosomal SNARE. Autophagy 9, 917–919. [PubMed: 23466629]

Jackson WT, 2015. Viruses and the autophagy pathway. Virology 479–480, 450–456.

Jägerström S, Polesie S, Wickström Y, Johansson BR, Schröder HD, Højlund K, Boström P, 2009. Lipid droplets interact with mitochondria using SNAP23. Cell Biol. Int. 33, 934–940. [PubMed: 19524684]

Karanasios E, Ktistakis NT, 2016. Autophagy at the Cell, Tissue and Organismal Level. Springer.

Kubo K, Kobayashi M, Nozaki S, Yagi C, Hatsuzawa K, Katoh Y, Shin H-W, Takahashi S, Nakayama K, 2015. SNAP23/25 and VAMP2 mediate exocytic event of transferrin receptor-containing recycling vesicles. Biol. Open 4, 910–920. [PubMed: 26092867]

Liu STH, Sharon-Friling R, Ivanova P, Milne SB, Myers DS, Rabinowitz JD, Brown HA, Shenk T, 2011. Synaptic vesicle-like lipidome of human cytomegalovirus virions reveals a role for SNARE machinery in virion egress. Proc. Natl. Acad. Sci. U. S. A. 108, 12869–12874. [PubMed: 21768361]

Messacar K, Abzug MJ, Dominguez SR, 2016. The Emergence of Enterovirus-D68. Microbiol Spectr 4. 10.1128/microbiolspec.EI10-0018-2016

Messacar K, Asturias EJ, Hixon AM, Van Leer-Buter C, Niesters HGM, Tyler KL, Abzug MJ, Dominguez SR, 2018. Enterovirus D68 and acute flaccid myelitis-evaluating the evidence for causality. Lancet Infect. Dis. 18, e239–e247. [PubMed: 29482893]

Mohamud Y, Shi J, Qu J, Poon T, Xue YC, Deng H, Zhang J, Luo H, 2018. Enteroviral Infection Inhibits Autophagic Flux via Disruption of the SNARE Complex to Enhance Viral Replication. Cell Rep. 22, 3292–3303. [PubMed: 29562184]

Monteiro-Brás T, Wesolowski J, Paumet F, 2019. Depletion of SNAP-23 and Syntaxin 4 alters lipid droplet homeostasis during *Chlamydia* infection. Microb. Cell Fact. 7, 46–58.

Morelli E, Ginefra P, Mastrodonato V, Beznoussenko GV, Rusten TE, Bilder D, Stenmark H, Mironov AA, Vaccari T, 2014. Multiple functions of the SNARE protein Snap29 in autophagy, endocytic, and exocytic trafficking during epithelial formation in Drosophila. Autophagy 10, 2251–2268. [PubMed: 25551675]

Ren H, Elgner F, Jiang B, Himmelsbach K, Medvedev R, Ploen D, Hildt E, 2016. The autophagosomal SNARE protein syntaxin 17 is an essential factor for the hepatitis C virus life cycle. J. Virol. 10.1128/JVI.00551-16

Richards AL, Jackson WT, 2012. Intracellular vesicle acidification promotes maturation of infectious poliovirus particles. PLoS Pathog. 8, e1003046. [PubMed: 23209416]

Richards AL, Soares-Martins JAP, Riddell GT, Jackson WT, 2014. Generation of unique poliovirus RNA replication organelles. MBio 5, e00833–13. [PubMed: 24570367]

Tabor-Godwin JM, Tsueng G, Sayen MR, Gottlieb RA, Feuer R, 2012. The role of autophagy during coxsackievirus infection of neural progenitor and stem cells. Autophagy 8, 938–953. [PubMed: 22751470]

Wong HH, Sanyal S, 2020. Manipulation of autophagy by (+) RNA viruses. Semin. Cell Dev. Biol. 101, 3–11. [PubMed: 31382014]

Yin K, Li Y, Ma Z, Yang Y, Zhao H, Liu C, Jin M, Wudong G, Sun Y, Hang T, Zhang H, Wang F, Wen Y, 2020. SNAP25 regulates the release of the Rabies virus in nerve cells via SNARE complex-mediated membrane fusion. Vet. Microbiol. 245, 108699. [PubMed: 32456820]

Zylbersztejn K, Galli T, 2011. Vesicular traffic in cell navigation. FEBS J. 278, 4497–4505. [PubMed: 21554543]

Research Highlights

- The cellular Qbc SNARE protein SNAP23 relocalizes from the plasma membrane to the cytosol after infection with EV-D68.
- SNAP23 knockdown induces the generation of large, electron-light vacuoles in the cytosol of cells. These vacuoles are still intact after infection.
- Loss of SNAP23 affects viral RNA replication and generation of viral replication organelles.
- These data lead us to suggest that the disruption of cellular trafficking brought on by lack of SNAP23 leads to cellular resources needed for building replication organelles being diverted into large vacuolar structures.

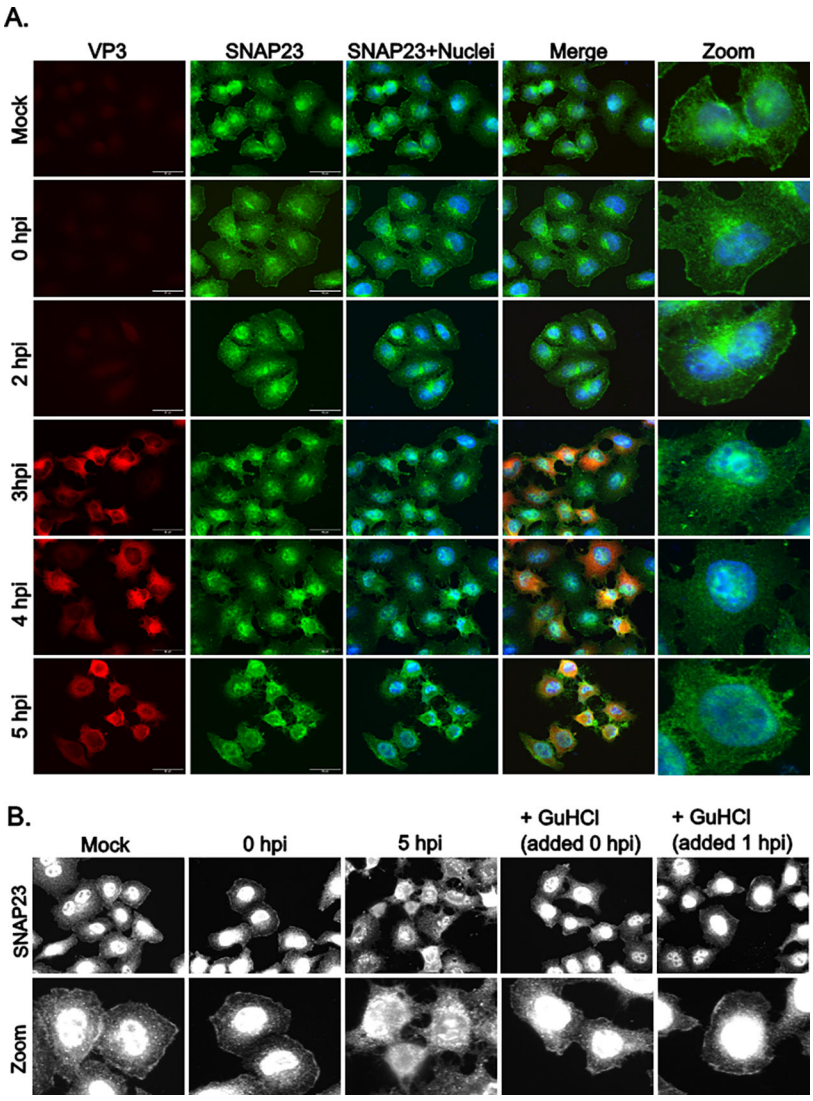

Figure 1. The Effects of EV-D68 Infection on SNAP23 Localization

(A) H1HeLa cells were infected with EV-D68 (MOI= 25) over a course of 5 hours. Cells were fixed and stained for immunofluorescence microscopy: SNAP23 (green), viral capsid protein VP3 (red), and nuclei (blue). Microscopy images shown are a representative set of images taken from one independent experiment. n = 3 independent experiments. Scale bar = 30 μm. (B) H1HeLa cells were infected with EV-D68 (MOI= 25) for 5 hours with no guanadine hydrochloride (GuHCl) added or with GuHCl (2 mM final concentration) added at 0 hpi or 1 hpi to inhibit active viral replication. An antibody against SNAP23 was used to visualize localization of SNAP23 during infection.

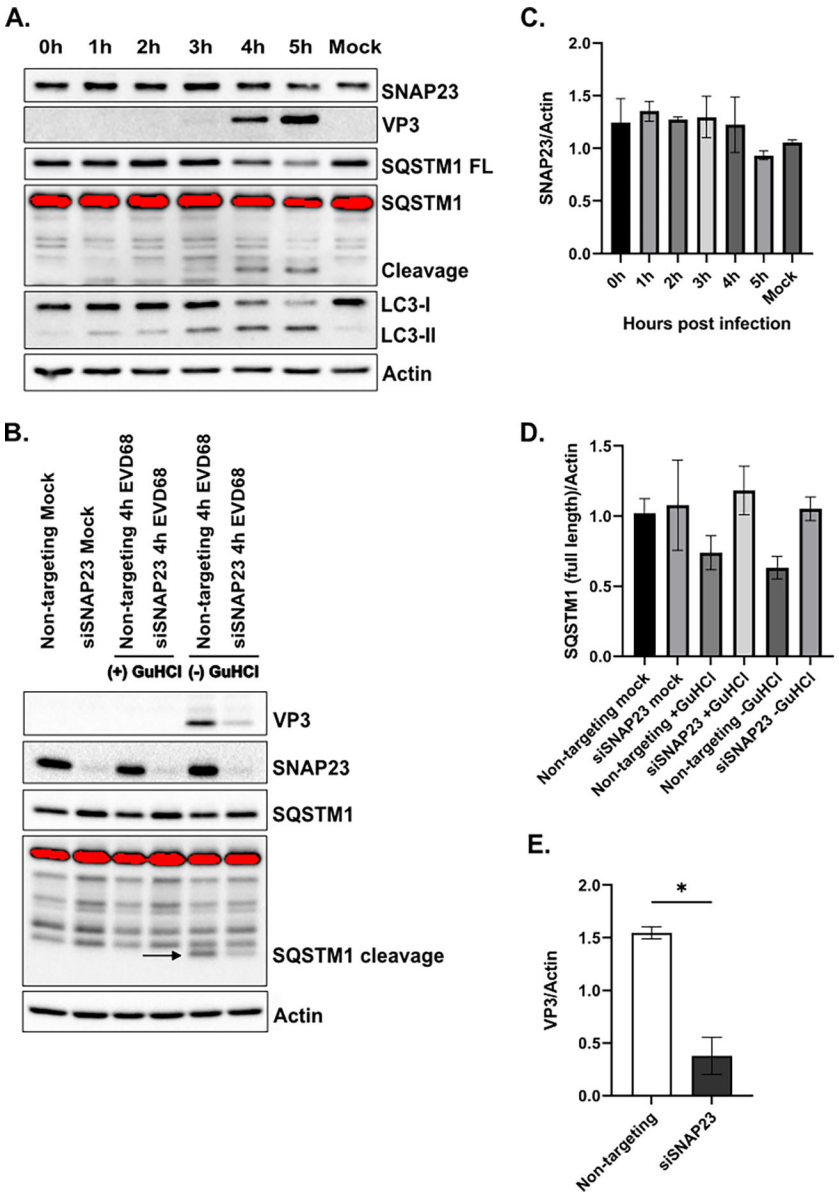

Figure 2. SNAP23 Expression is not Altered by EV-D68 Infection but SNAP Knockdown Inhibits VP3 Expression

(A) Cells were infected with EV-D68 over a course of 5 hours (MOI =25). Samples were collected at each indicated time point for Western blot analysis. (B) Cells were transfected with non-targeting or SNAP23 siRNAs for 48 hours and then infected with EV-D68 (MOI=10) for 4 hours. Cell lysates were collected at the end of the infection and used for Western blot analysis. Subsets of non-targeting and siSNAP23 transfected cells in B were also treated with 2mM guanidine hydrochloride (GuHCl) as a control to inhibit viral replication. (C) SNAP23 bands from three independent experiments, completed for (A), were semi-quantified and normalized to beta-actin. (D) Bands from full length SQSTM1, in (B), were semi-quantified from three independent experiments and normalized to beta-actin. (E) VP3 bands were semi-quantified from three independent experiments and independent from the blots, in (B), probed against SQSTM1 due to the cleavage product from SQSTM1

is close in size to VP3. n= 3 independent experiments. Unless noted by an asterisk, results were otherwise not statistically significant. *=p-value <0.05 and error bars represent the mean ±SEM.

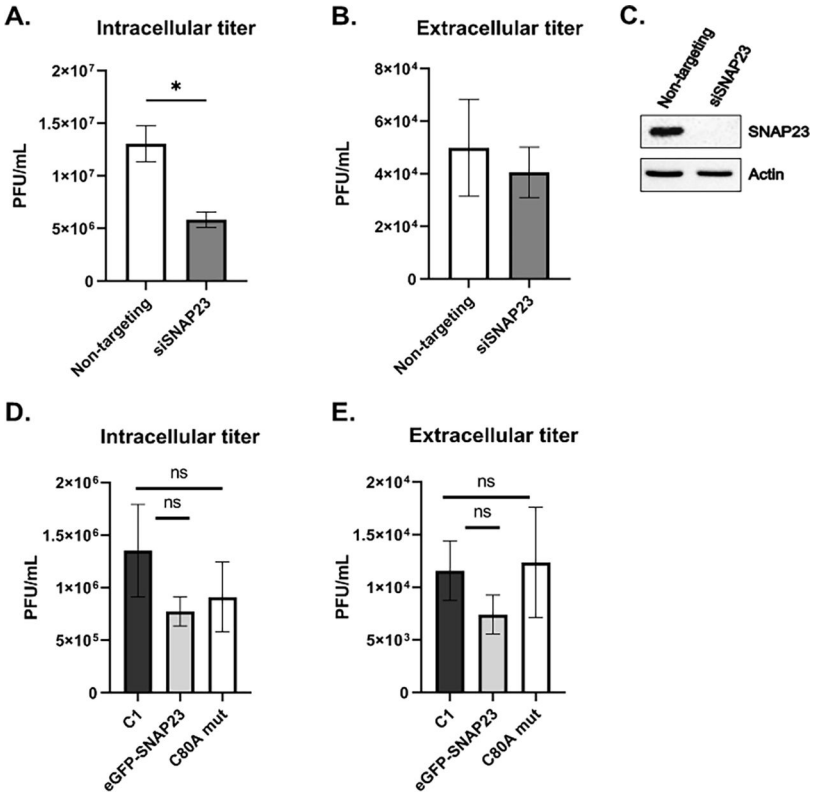

Figure 3. SNAP23 is Involved with EV-D68 Replication but not Egress.

H1HeLa cells were either transfected with non-targeting siRNA or SNAP23 siRNAs for 48 hours. After transfection, cells were infected with EV-D68 at an MOI of 0.1 for 6 hours. Samples were collected and intracellular (A) and extracellular (B) titers were measured by plaque assay. (C) SNAP23 knockdown efficiency was measured by Western blot analysis. Intracellular (D) and extracellular (E) titers were measured by plaque assay after H1HeLa cells were transfected for 20 hours to overexpress SNAP23 or a SNAP23 mutant (C80A), and compared to a GFP control. n = 4 independent experiments (A and B), n = 3 independent experiments (D and E). * = p-value < 0.05, ns = not significant, and error bars represent the mean ±SEM.

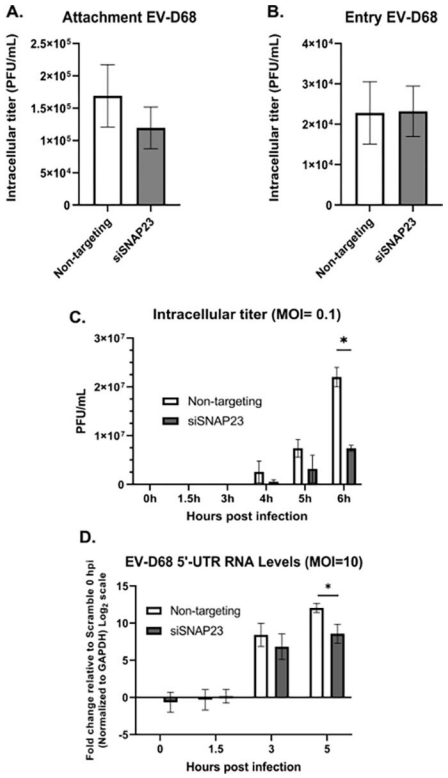

Figure 4. SNAP23 Affects EV-D68 Post-Entry

(A) After non-targeting or SNAP23 siRNA treatment for 48 hours, cells were prechilled at 4°C for 1hr, underwent viral adsorption with EV-D68 (MOI= 30) for 1 hour at 4°C, washed thoroughly, and collected to titer by plaque assay to assess viral attachment. (B)To assess viral entry, cells underwent a similar method of chilling and viral adsorption, in addition to a 1 hr infection at 37°C before washing and sample collection for titering. Results for A and B showed no significant differences between non-targeting control and the SNAP23 knockdown. (C) H1HeLa cells were infected with EV-D68 over a course of 5 hours (0, 1.5, 3, 4, and 5 hours; MOI = 10) after transfection of non-targeting or SNAP23 siRNAs for 48 hours. Intracellular samples were collected for titering by plaque assay. (D) Under the same conditions and time points at 0, 1.5, 3, and 5 hours, samples were collected for qPCR analysis to assess viral RNA levels of the 5'UTR for EV-D68. Data represents relative expression of 5'UTR where samples are compared to the 0 h non-targeting condition. All samples are normalized to GAPDH and have been log2 transformed. Data presented in A and B; n= 4 independent experiments. Data represented in C and D; n=3 independent experiments. * = p-value < 0.05 and error bars represent the mean ±SEM. Unless noted by an asterisk, results were otherwise not statistically significant.

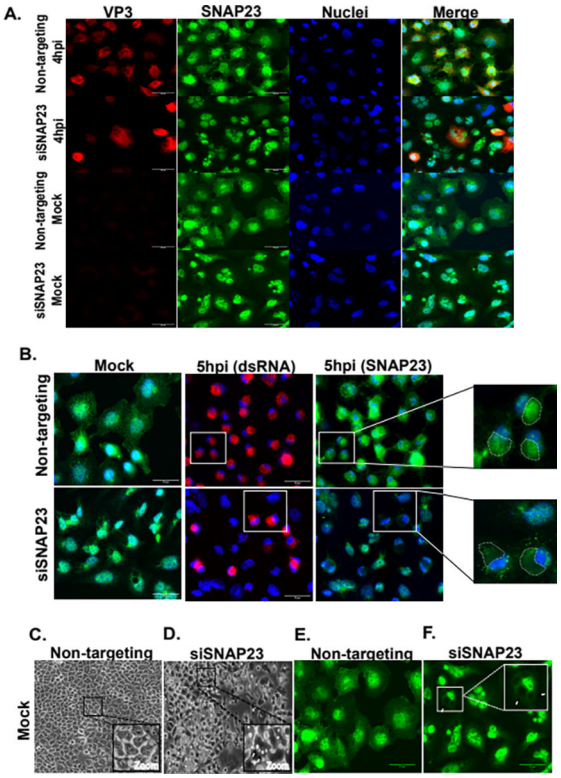

Figure 5. SNAP23 is Necessary for Viral RNA Replication

(A) H1HeLas were transfected with non-targeting siRNA or SNAP23 siRNAs for 48 hours and then infected with EV-D68 for 4 hours (MOI = 10). Cells were stained for SNAP23 (green), viral capsid protein VP3 (red), and nuclei (blue). (B) non-targeting and SNAP23 siRNAs were transfected in H1HeLa cells for 48 hours. Cells were then infected with EV-D68 (MOI = 10) for 5 hours and then fixed and stained against dsRNA (red), nuclei (blue), and SNAP23 (green). Boxed areas show a set of cells that express and do not express dsRNA. The zoomed-in panels show the same subset of cells with the cytosolic SNAP23 outline in white dots. Adjustments have been made to the contrast and brightness to better show the cytosolic SNAP23. (C) Phase contrast/light microscopy image of H1HeLa cells that have been transfected with non-targeting siRNA for 48 hours, with no infection. (D) Phase contrast/light microscopy image of H1HeLa cells that have been transfected with SNAP23 siRNAs for 48 hours, with no infection. (E) Immunofluorescent microscopy image of H1HeLa cells transfected with non-targeting siRNA, with mock infection, and stained against SNAP23, under the oil immersion objective. (F) Immunofluorescent microscopy image of H1HeLa cells transfected with SNAP23 siRNAs, with mock infection, and stained against SNAP23. The white arrows in D and F indicate where large spaces in the cells are located during SNAP23 knockdown. n = 3 independent experiments; scale bars = 30 μm. Microscopy images shown are a representative set of images taken from one independent experiment.

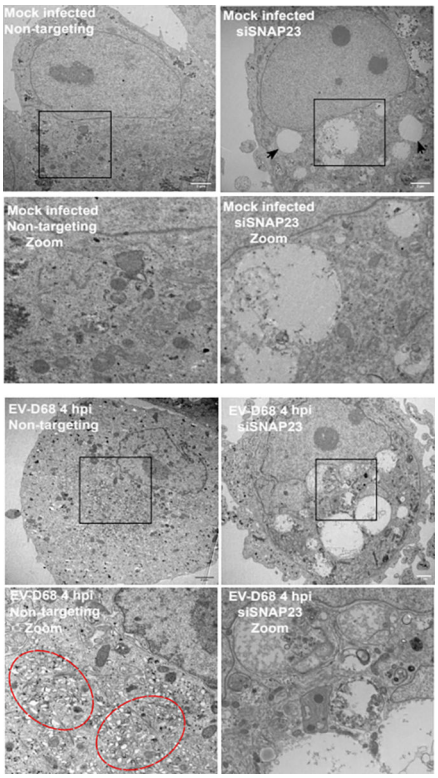

Figure 6. SNAP23 Knockdown Generates Large Vacuoles and Occludes Formation of Viral Replication Organelles

Transmission electron micrographs of H1HeLa cells transfected either with non-targeting or SNAP23 siRNAs, with mock infection or a 4 hour infection with EV-D68 (MOI = 10). Black boxes in the top panel are zoomed in and displayed in the bottom panel. Black arrows indicate the location of the electron light/large empty spaces seen in SNAP23 knockdown cells. Red dotted ovals show the areas where replication organelles are located in infected cells. Scale bar = 2 μm. TEM images are representative of one biological experiment.

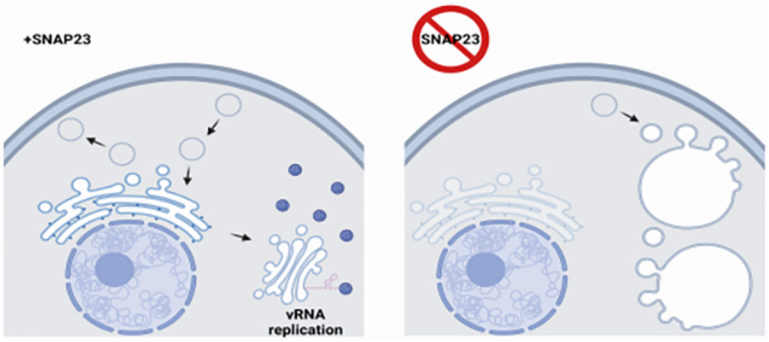

Figure 7. Model of Hypothesized Role of SNAP23 during EV-D68 Replication.

SNAP23 is important for generating viral replication organelles. In the absence of SNAP23, large (4–6μm diameter) electron-light vacuoles are observed. We hypothesize that these vacuoles result from breakdown in normal endocytic trafficking normally mediated by SNAP23. In this model, resources needed to generate viral replication organelles are not available due to breakdown of endocytic recycling, resulting in the large vacuoles. The reduction in virus production is largely due to a resultant reduction in vRNA replication. Model created with BiorRender.com.